

Analytical calculation of the Peierls-Nabarro barriers for the Remoissenet-Peyrard substrate potential

David Yemélé^{1,2} and Timoléon C. Kofané^{1,3}¹Laboratoire de Mécanique, Faculté des Sciences, Université de Yaoundé I, BP 812, Yaoundé, Cameroun²Département de Physique, Faculté des Sciences, Université de Dschang, BP 67, Dschang, Cameroun³Laboratoire de Physique de l'Université de Bourgogne, avenue Alain Savary, BP400, 21011 Dijon, France

(Received 30 December 1999; revised manuscript received 13 March 2000; published 23 July 2002)

We derive analytically the pinning potential and the pinning barrier of kinks due to discreteness of lattices for the Remoissenet-Peyrard substrate potential by means of the residue method. The theoretical analysis in the low discreteness effect regime is compared in detail with numerical results of Peyrard and Remoissenet [Phys. Rev. B **26**, 2886 (1982)], yielding a very satisfactory agreement.

DOI: 10.1103/PhysRevE.66.016606

PACS number(s): 41.20.Jb, 05.45.-a

I. INTRODUCTION

The influence of lattice discreteness on the properties of nonlinear systems having kink solutions was investigated by several authors [1–4]. These studies have pointed out a large variety of effects, including modification of soliton velocity and its form and leading sometimes to the pinning of the soliton on the lattice. In certain systems such as incommensurate systems [5,6], the discreteness effects bring not only a quantitative change with respect to the continuum model but also a qualitative change: the discrete lattice causes the distortion in the incommensurate phase to be both modulated and pinned to the lattice, preventing a truly incommensurate phase from arising and causing the appearance of a gap in the phason spectrum [5]. Note that except for some numerical investigations [7] and the approximated investigations [8,9] on the deformable sine-Gordon potential of Remoissenet and Peyrard [10], the discrete models that were used to describe domain walls, incommensurate systems, or adsystems were restricted to the discretized version of the ϕ^4 and sine-Gordon (sG) models [11–13].

However the deformable potential of Remoissenet and Peyrard plays an important role in atomic chains. Its use in the present work is dictated by our effort to go beyond the mathematical problem and obtains results that may be useful for real materials that undergo structural changes such as shape distortions, variations of crystalline structures, or conformational changes in some of their physical parameters. Such materials cannot be satisfactorily described by substrate potentials with constant parameters, for which much work has already been done in the context of their dynamical behavior. Also it is important to note that the Remoissenet-Peyrard substrate potential has been used to describe diffusion of adatoms [14] as a model for reconstructive surface growth [15], and to describe the complicated exchange-mediated diffusion mechanism [16]. It has also been used to calculate the diffusion coefficient of adsorbates in metallic substrates [9] and the nucleation rate of kink-antikink pairs at low temperature [17]. Finally, the deformable spin model Hamiltonian has been recently introduced [18], to name only a few.

Our aim in this paper is to derive the exact analytical

result of the pinning potential, the well-known Peierls-Nabarro (PN) potential, in the Remoissenet-Peyrard (RP) model [10], in the limits where dressing corrections of the kink profile are negligible. This parameter is very important for many physical applications in which nonlinear excitations are invoked to describe real systems. We recover the behavior predicted numerically by Peyrard and Remoissenet [7]. The results are presented here in the context of dislocation theory but they are also applicable to many other physical systems outlined in the preceding paragraph. We first present the basic results of the continuum model in Sec. II, and second, in Sec. III, we use the reduced Lagrangian approach to derive the equation of motion for the center of mass of the kink. The PN barrier is also calculated. Finally, Sec. IV is devoted to concluding remarks.

II. MODEL DESCRIPTION

To begin, let us consider a system of particles of mass m harmonically coupled and placed on an infinite one-dimensional (1D) lattice of spacing a . The system is governed by the discrete Lagrangian

$$L = T - U, \quad (1)$$

where the kinetic and potential energies are, respectively, given by

$$T = Aa \sum_i \frac{1}{2} \dot{\phi}_i^2 \quad (2)$$

and

$$U = Aa \sum_i \left\{ \frac{C_0^2}{2a} (\dot{\phi}_{i+1} - \dot{\phi}_i)^2 + \omega_0^2 V(\phi_i) \right\}, \quad (3)$$

where the overdot indicates the time derivative. The constant $A \approx ma$ sets the energy scale of the system, and C_0 and ω_0 are characteristic velocity and frequency, respectively. ϕ_i is the scalar dimensionless longitudinal displacement of the i th particle on a 1D lattice. The nonlinear “one-site potential” $V(\phi_i)$ is an external potential, representing the combined influence of the surrounding crystal or macromolecule

and external effects, such as an electric or magnetic field. We concentrate our attention on that introduced by Remoissenet and Peyrard (RP) [10],

$$V(\phi_i) = (1-r)^2 \frac{1 - \cos \phi_i}{1 + r^2 + 2r \cos \phi_i}, \quad (4)$$

where $|r| < 1$. As r varies, the amplitude of the potential remains constant with degenerate minima $2\pi n$ and maxima $(2n+1)\pi$, while its shape changes. At $r=0$, the model reduces to the well-known sG model.

In the continuum soliton limit, the system described by the Lagrangian (1) possesses kink solutions $\phi(x - vt) \equiv \phi(s)$, verifying the differential equation

$$\frac{1}{2} \left(\frac{d\phi}{ds} \right)^2 = \frac{\gamma^2}{d_0^2} V(\phi), \quad d_0 = c_0/\omega_0, \quad \gamma = (1 - v^2/c_0^2)^{-1/2}, \quad (5)$$

where d_0 is the characteristic length scale of the system, γ is the Lorentz contraction factor, and x is the continuum space variable with $x = ia$, while v is the velocity. From Eq. (5), one obtains two families of implicit kink solutions [10]:

$$\frac{\gamma s}{d_s^{(1)}} = \pm \operatorname{sgn}(\phi - \pi) \left\{ \frac{(1 - \alpha^2)^{1/2}}{\alpha} \tan^{-1} \left[\frac{(1 - \alpha^2)^{1/2}}{\alpha^2 + \tan^2(\phi/2)} \right]^{1/2} + \tanh^{-1} \left[\frac{\alpha^2}{\alpha^2 + \tan^2(\phi/2)} \right]^{1/2} \right\}, \quad (6a)$$

with $d_s^{(1)} = d_0 \alpha$ and for $-1 < r \leq 0$,

$$\frac{\gamma s}{d_s^{(2)}} = \pm \operatorname{sgn}(\pi - \phi) \left\{ (1 - \alpha^2)^{1/2} \tanh^{-1} \left[\frac{1 - \alpha^2}{1 + \alpha^2 \tan^2(\phi/2)} \right]^{1/2} - \tanh^{-1} \left[\frac{1}{1 + \alpha^2 \tan^2(\phi/2)} \right]^{1/2} \right\}, \quad (6b)$$

with $d_s^{(2)} = d_0/\alpha$ and for $0 \leq r < 1$, where $\alpha = (1 - |r|)/(1 + |r|)$. The sign (+) corresponds to the kink solution while the sign (−) corresponds to the antikink solution. The kink rest energy (E_s) and rest mass (M_s) are given by

$$E_s^{(\ell)} = 8A c_0 \omega_0 G^{(\ell)}(r) \quad \text{and} \quad M_s^{(\ell)} = \frac{8A}{d_0} G^{(\ell)}(r), \quad \ell = 1, 2, \quad (7)$$

with

$$G^{(1)}(r) = (1 - \alpha^2)^{1/2} \tan^{-1} \left[\frac{(1 - \alpha^2)^{1/2}}{\alpha} \right],$$

$$G^{(2)}(r) = \alpha (1 - \alpha^2)^{1/2} \tanh^{-1} [(1 - \alpha^2)^{1/2}], \quad (8)$$

where the superscripts “(1)” and “(2)” stand for $-1 < r \leq 0$ and $0 \leq r < 1$, respectively. The parameters $d_s^{(\ell)}$ ($\ell = 1, 2$) are the “pseudo-kink-width” [10]. For $r=0$, Eqs. (6) reduce to the usual sG kink. When r tends to 1, $d_s^{(2)}$ tends to infinity. On the other hand, when r decreases and tends to -1 , $d_s^{(1)}$ tends to zero. Thus, the kink extension is not only deter-

mined by the characteristic length scale d , but also by the curvature of the minima of the potential [19]. It is important to note that when r tends to -1 , even if the neighboring particles are sufficiently closed (strong coupling), the kink extension could be just a few lattice spacings and, consequently, the discreteness effects on soliton dynamics and thermodynamics properties could not be neglected [20].

III. CALCULATION OF THE PINNING POTENTIAL

In order to analyze the influence of the lattice effects on the kink dynamics, we use the ansatz $\phi_i = \phi(ia - X(t)) \equiv \phi_i(X(t))$, where the dynamical variable $X(t)$ represents the position of the center of mass of the kink. $\phi_i(X(t))$ are the continuum soliton solutions [Eq. (6)] at the site i and the discrete corrections or dressing of the continuum solitons for the radiated phonons emitted by solitons during their propagation are assumed to be small. This approximation limits the range of validity only for $d_0 > a$. In the continuum limit, $X(t)$ is proportional to time [e.g., $X(t) = vt$, where v is the kink velocity] but this is not the case in the discrete lattice, where the translational invariance of kink motion is broken by the periodic variation of the kink parameter.

Substituting $\phi_i(X(t))$ into the Lagrangian (1), we obtain the reduced form

$$L = \frac{1}{2} M_s \dot{X}^2 - U(X), \quad (9)$$

where M_s defined by

$$M_s = Aa \sum_i \left(\frac{\partial \phi_i}{\partial X} \right)^2 \quad (10)$$

is the effective mass of the kink. The potential energy $U(X)$ depends on X through $\phi_i(X(t))$. With the use of the continuum limit and the differential equation (5), it appears that the potential energy $U(X)$ is given by

$$U(X) = 2Aa\omega_0^2 \sum_i V[\phi_i(X)], \quad (11)$$

where $V(\phi)$ is the underlying potential of the system defined in Eq. (4). Also the effective kink mass can be rewritten in a more suggestive form as

$$M_s = \frac{2Aa}{d_0^2} \sum_i V[\phi_i(X)]. \quad (12)$$

The numerical computation of these two expressions shows a periodic variation with X , with period proportional to the lattice constant a . According to this result, we use the Fourier series expansion to write

$$\sum_i V[\phi_i(X)] = \frac{A_0}{2} + \sum_{n=1}^{\infty} \left[\alpha_n \cos\left(\frac{2\pi n X}{a}\right) + b_n \sin\left(\frac{2\pi n X}{a}\right) \right] \quad (13)$$

with

$$a_n = \frac{2}{a} \int_0^a \sum_i V[\phi_i(X)] \cos\left(\frac{2\pi n X}{a}\right) dX, \quad (14)$$

$$b_n = \frac{2}{a} \int_0^a \sum_i V[\phi_i(X)] \sin\left(\frac{2\pi n X}{a}\right) dX.$$

This summation (13) can be rewritten as

$$\sum_i V[\phi_i(X)] = \frac{A_0}{2} + \sum_{n=1}^{\infty} |\tilde{A}_n| \cos\left(\frac{2\pi n X}{a} + \varphi_n\right), \quad (15)$$

where a_n and b_n are the real and imaginary parts of \tilde{A}_n with modulus $|\tilde{A}_n|$. Hence \tilde{A}_n is given by

$$\tilde{A}_n = a_n + j b_n = \frac{2}{a} \int_0^a \sum_{i=1}^N V[\phi_i(X)] e^{-(2\pi n X/a)j} dX. \quad (16a)$$

By using the transformation $Z = ia - X$, Eq. (16a) becomes

$$\begin{aligned} \tilde{A}_n &= -\frac{2}{a} \sum_{i=-(N-1)/2}^{(N-1)/2} \int_{ia}^{(i-1)a} V[\phi(Z)] e^{j(2\pi n Z/a)} dZ \\ &= -\frac{2}{a} \left\{ \int_{-(N-1)/2-1}^{(N-1)/2} + \int_{-(N-1)/2}^{(N-1)/2+1} + \dots \right. \\ &\quad \left. + \int_{(N-1)/2-1}^{(N-1)/2} \right\} V[\phi(Z)] e^{j(2\pi n Z/a)} dZ, \end{aligned} \quad (16b)$$

which reduces to (with $N \rightarrow \infty$)

$$\tilde{A}_n = \frac{2}{a} \int_{-\infty}^{+\infty} dZ V[\phi(Z)] e^{j(2\pi n Z/a)}. \quad (17a)$$

Also φ_n is defined by

$$\varphi_n = \tan^{-1} \left(\frac{-b_n}{a_n} \right) = \arg(\tilde{A}_n). \quad (17b)$$

It appears from Eqs. (13), (17), and (22) that the problem of the calculation of the potential energy and the kink mass in the discrete system is reduced to that of the integration of the quantity

$$Q_n = \int_{-\infty}^{+\infty} dZ V[\phi(Z)] \exp(j2\pi n Z/a) \quad (18)$$

since $\tilde{A}_n = (2/a)Q_n$. We can evaluate it either by the saddle-point method or by knowing the residues of the integrand associated with poles located in the above half-plane since $V[\phi(Z)]$ tends to zero when Z tends to $\pm\infty$. When one relies upon the residue method, the problem is to find the singular points of the function $V[\phi(Z)]$. These singular points, which in this case are branch points, are located at

$$\begin{aligned} \phi_{s1} &= \pm j \ln[(1-\alpha)/(1+\alpha)] + 2m\pi, \\ \phi_{s2} &= \pm j \ln[(1-\alpha)/(1+\alpha)] + (2m+1)\pi, \end{aligned} \quad (19)$$

where m is an integer. These points correspond in the z plane to

$$Z_m^{(2)} = \lambda(1+2m) \quad \text{and} \quad Z_m^{(1)} = (\lambda_1 + j\lambda_2)(1+2m) \quad (20a)$$

with

$$\begin{aligned} \lambda_1 &= (d_0\pi/2)(1-\alpha^2)^{1/2}, \quad \lambda_2 = (d_0\pi/2)\alpha, \\ \lambda &= (d_0\pi/2)\alpha/[1+(1-\alpha^2)^{1/2}] \end{aligned} \quad (20b)$$

obtained by substituting Eqs. (19) into the implicit kink solution (6). From the residues theorem

$$Q_n = \int_{-\infty}^{+\infty} F(Z) dZ = 2\pi j \sum_{m=0}^{\infty} R(Z_m, F), \quad (21a)$$

where $R(Z_m, F)$ is the residue of the function $F(Z)$ at $Z = Z_m$, we obtain after some lengthy calculation

$$Q_n^{(1)} = (4\pi^2 d_0^2 n/a) \frac{\sinh(2\pi n \lambda_2/a) \cos(2\pi n \lambda_1/a) + j \sin(2\pi n \lambda_1/a) \cosh(2\pi n \lambda_2/a)}{\sinh^2(2\pi n \lambda_2/a) + \sin^2(2\pi n \lambda_1/a)} G^{(1)}(r), \quad (21b)$$

$$Q_n^{(2)} = (4\pi^2 d_0^2 n/a) \frac{\alpha}{[1+(1-\alpha^2)^{1/2}] \sinh(2\pi n \lambda/a)} G^{(2)}(r), \quad (21c)$$

where $G_{(r)}^{(1)}$ are the numerical constants depending on the potential defined in Eq. (8). The fundamental harmonic is readily calculated and yields

$$A_0^{(\ell)} = \frac{8d_0}{a} G^{(e)}(r), \quad \ell = 1, 2. \quad (22)$$

With the help of Eqs. (11), (12), (15), and (16), the potential energy and the kink effective mass can be evaluated.

For example, substituting \tilde{A}_n into Eq. (15) and the resulting equation (15) into Eq. (11) yields the potential energy

$$U^{(\ell)}(X) = E_s^{(\ell)} + \sum_{n=1}^{\infty} U_n^{(\ell)} \cos\left(\frac{2\pi n X}{a} + \varphi_n^{(\ell)}\right) \quad (23)$$

with

$$U_n^{(1)} = \frac{16\pi^2 d_0^2 \omega_0^2 A}{a} \frac{nG^{(1)}(r)}{[\sinh^2(2\pi n\lambda_2/a) + \sin^2(2\pi n\lambda_1/a)]^{1/2}}, \quad (24a)$$

$$\tan \varphi_n^{(1)} = \frac{\tan(2\pi n\lambda_1/a)}{\tanh(2\pi n\lambda_2/a)}, \quad (24b)$$

and

$$U_n^{(2)} = \frac{16\pi^2 A d_0^2 \omega_0^2}{a} \frac{n\alpha G^{(2)}(r)}{[1 + (1 - \alpha^2)^{1/2}] \sinh(2\pi n\lambda/a)}, \quad (24c)$$

$$\tan \varphi_n^{(2)} = 0. \quad (24d)$$

Similarly, the substitution of Eq. (15) into Eq. (12) yields the effective kink mass:

$$M_s^{(\ell)}(X) = M_s^{(\ell)} + \sum_{n=1}^{\infty} M_{sn}^{(\ell)} \cos\left(\frac{2\pi nX}{a} + \varphi_n^{(\ell)}\right) \quad (25)$$

with

$$M_{sn}^{(1)} = \frac{16\pi^2 A}{a} \frac{naG^{(1)}(r)}{[\sinh^2(2\pi\lambda_2 n/a) + \sin^2(2\pi\lambda_1 n/a)]^{1/2}}, \quad (26a)$$

$$M_{sn}^{(2)} = \frac{16\pi^2 A}{a} \frac{naG^{(2)}(r)}{[1 + (1 - \alpha^2)^{1/2}] \sinh(2\pi n\lambda/a)}. \quad (26b)$$

The parameters $M_s^{(\ell)}$ and $E_s^{(\ell)}$ that appear in Eqs. (23) and (25) are the kink rest mass and kink rest energy in the continuum limit [10], respectively, defined by Eq. (7). In this limit, these quantities are constant parameters. However, in the discrete lattices, these parameters depend on the kink position in the lattice. Therefore, it appears that the discrete lattice is the source of periodic modulation of kink parameters (mass and energy) as the kink propagates along the lattice. As a consequence, a kink in the discrete lattice has a periodically varying effective mass and moves in a periodic potential energy.

Equation (23) represents the total potential energy of the discrete system and can be regarded as the Peierls-Nabarro energy, while Eq. (25) represents the effective kink mass when $r > 0$, and the phase $\varphi_n^{(2)}$ in the argument of the cosine term is zero. Due to the presence of the hyperbolic sine function in the denominator of $U_n^{(2)}$, the harmonics of second order and more are negligible. Then, $U^{(\ell)}(X)$ reduces to

$$U^{(2)}(X) = E_s^{(2)} + U_1^{(2)} \cos\left(\frac{2\pi X}{a}\right). \quad (27)$$

Also, the kink effective mass has the same behavior,

$$M_s^{(2)}(X) = M_s^{(2)} + M_{s1}^{(2)} \cos\left(\frac{2\pi X}{a}\right). \quad (28)$$

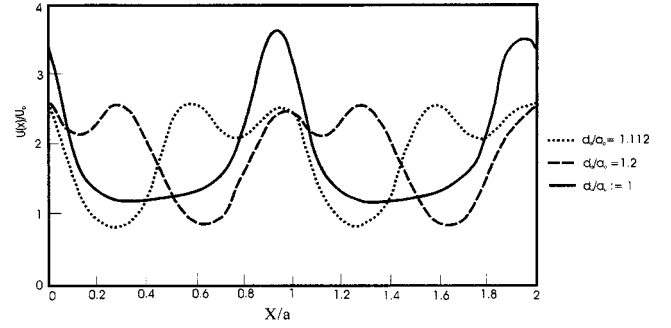


FIG. 1. Pinning potential $U(X)/U_0$ in dimensionless unit ($U_0 = Ac_0\omega_0$) as a function of X/a in two unit cells for $r = -0.7$ and different values of the discretization parameter d_0/a .

However, since $M_s^{(2)} \gg M_{s1}^{(2)}$, the kink mass $M_s^{(2)}(X)$ is reduced to its fundamental harmonic $M_s^{(2)}$. When $r < 0$, one notes the presence of the sine term in the $M_n^{(1)}$ expression and the phase $\varphi_n^{(1)}$ in the cosine term of both the potential $U^{(1)}(X)$ and the mass $M_n^{(1)}(X)$. It appears that, in the system with large length scale ($d_0 \gg a$) and/or for the substrate potential close to the sine-Gordon one ($r \rightarrow 0$), the hyperbolic sine function in the denominator of $U_n^{(1)}$ dominates the sine function, thus the harmonic of order more than 2 is negligible. Hence

$$U^{(1)}(X) = E_s^{(1)} + U_1^{(1)} \cos(2\pi X/a + \varphi_1^{(1)}) \quad (29)$$

and the kink mass is reduced to its fundamental harmonic $M_s^{(1)}$ (since $M_s^{(1)} \gg M_{s1}^{(1)}$). However, when the system is highly discrete ($d_0/a \leq 1$) and/or for the substrate potential with a very sharp bottom or flat top ($r \rightarrow -1$), the hyperbolic sine function in the denominator of $U_n^{(1)}$ tends to zero and the sine function predominates. In this case, the harmonic of order more than 1 dominates the harmonic of order 1. Thus, the potential presents more than one minima within one unit cell. Figure 1 illustrates this behavior and shows examples of the variations of the PN potential $U(X)$ for different values of d . The PN potential (23) can no longer be satisfactorily described by the approximate equations (27) and (29).

Next we consider the pinning barrier. Note that the periodic modulation of the potential $U^{(\ell)}(X)$ as the kink propagates along the lattice is the source of the periodic pinning potential experienced by this kink. The amplitude of this potential energy is the well-known PN barrier E_{PN} [1]. In the case of a substrate potential with a flat bottom ($r > 0$), this barrier can be accurately deduced from Eq. (27). It yields

$$E_{PN}^{(2)} = 2U_1^{(2)}. \quad (30)$$

When $r < 0$, but still greater than -0.5 and/or the length scale $d_0 > a$ (weak discrete system), the PN barrier is also given by

$$E_{PN}^{(1)} = 2U_1^{(1)}, \quad (31)$$

which is deduced from Eq. (29). When the kink kinetic energy is not sufficient, it can be trapped by the PN potential, after which it oscillates in the PN equilibrium site with the PN frequency with PN defined as follows:

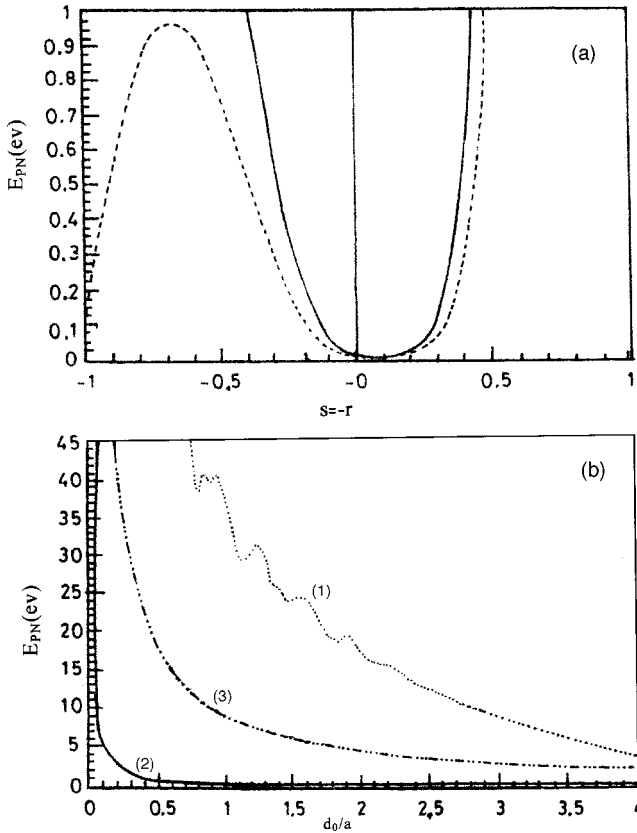


FIG. 2. Variation of the pinning barrier E_{PN} , in eV, with the parameter of hydrogen adsorbed on a tungsten surface ($a=3 \text{ \AA}$, $m=1 \text{ uma}$, $c_0=5208 \text{ m/s}$, $\omega_0=3 \times 10^{13} \text{ rd/s}$; see Ref. [17]), as a function of [dashed curve is the truncated result obtained from Eqs. (30) and (31) while the full curve is the result of Eq. (33)] (a) deformable parameter r with $d_0/a=1.5$, (b) dimensionless discretization parameter d_0/a for three values of deformable parameter: (1) $r=-0.7$; (2) $r=0$; and (3) $r=+0.7$.

$$(\omega_{PN}^{(2)})^2 = \frac{4\pi^2 U_1^{(2)}}{a^2 M_s^{(2)}}. \quad (32)$$

Moreover, when $r < 0.5$ and/or $d_0 \leq a$ (highly discrete system), the PN barrier is given by

$$E_{PN}^{(\ell)} = \max[U^{(\ell)}(X)] - \min[U^{(\ell)}(X)], \quad (33)$$

where $\max[U^{(\ell)}(X)]$ and $\min[U^{(\ell)}(X)]$ are the maximum and the minimum values of $U^{(\ell)}(X)$ when X varies from zero to a , respectively. Here, one must take into account the high harmonic of the PN potential in the calculation of the PN potential. Figure 2 shows the variations of E_{PN} as a function of the deformable parameter r , which determines the shape of the substrate potential. It appears that the discreteness effects strongly depend on the shape of the substrate potential. They are minimal for the sine-Gordon profile ($r=0$), but increase rapidly when the shape of the potential becomes more abrupt (either with a sharp or flat top). It is important to note that for $r > 0$, the spatial extension of the kink is $d_s^{(2)} = d_0/a$ so that, when $r \rightarrow 1$, very large kinks are needed to avoid discreteness effects.

We now turn our attention to a qualitative and quantitative comparison of our theoretical results with the numerical simulations of Peyrard and Remoissenet [7]. In fact, Peyrard and Remoissenet have calculated numerically the pinning potential and pinning barrier in the RP model and pointed out the following.

First, the shape of the pinning potential by the moving kink depends on the shape of the one-site potential; it is sinusoidal in the case of the sG potential shape with a spatial periodicity equal to the lattice constant as assumed by Currie *et al.* [20], and may exhibit two minima within a unit cell in the case of the RP potential. This aspect of their results can be interpreted by Eq. (23). Figure 1 illustrates this behavior. However, Fig. 1 shows that the periodicity of the pinning potential is still equal to the lattice constant. This failure can be justified by the fact that the appearance of two minima with equal magnitude within a unit cell is obtained in the highly discrete system. So, in the high discreteness effect regime, we do not have analytical solutions for the discrete RP model.

Second, the magnitude of the discreteness effects is strongly dependent on the shape of the substrate potential, their variation as a function of the discretization parameter d_0 is also very sensitive to the shape of the substrate potential, and that very large kink may be pinned by discreteness effects. Here also, these results can be interpreted by Eq. (23). Figure 2 is an example of this illustration.

Finally, there is no oscillation in the pinning barrier E_{PN} , where $r \geq 0$, and as d_0 increases E_{PN} decreases. However, when $r < 0$, there appears an oscillation in E_{PN} . For this, our result [see Eq. (21)] shows an oscillatory behavior of E_{PN} as a function of d_0 with a pseudoperiod proportional to $2a/\pi\sqrt{1-\alpha^2} = 2a(1+|r|)/\pi\sqrt{4|r|}$.

Hence, substantial aspects of the results of Peyrard and Remoissenet [7] have been obtained. However, due to the fact that we have neglected the dressing correction of the kink profile in the lattice, the result is limited in the range where the continuum soliton profile can be obtained. If we assume that the discreteness parameter is given by the kink width $d^{(1)}$, for negative values of r , the range of validity of our result $d^{(1)} > a$ yields $|r| < [(d_0/a) - 1]/[(d_0/a) + 1]$.

IV. CONCLUSION

In summary, we have studied analytically the discreteness effects on the kink dynamics of a one-dimensional system with the RP substrate potential. The PN potential has been derived. It turns out that the discreteness effect depends not only on the kink width, but also on the shape of the substrate potential. In the substrate with a sharp bottom ($r > 0$), the pinning barrier can be accurately approximated by the amplitude of the first harmonic of the Fourier series expansion of the pinning potential, but the shape of this potential may deviate from the sinusoidal one. Also, when the substrate potential has a flat bottom with deformable parameter $r < 0.5$, this approximation is still valid. However, when $r < 0.5$ this approximation may fail, and one should take into

account the higher harmonics in the analytical expression of the PN potential. The higher harmonic terms may contribute significantly to increase the value of the PN barrier. Despite the significant results obtained in this paper, it would be

interesting and more accurate to pursue the study of the discreteness effects by taking into account the dressing of the kink. The account of this problem leads to noticeable modification of the kink profile and dynamics.

-
- [1] F. Nabarro, in *Theory of Crystal Dislocations* (Clarendon, Oxford, 1967).
- [2] C. R. Willis, M. El-Batanouny, and P. Stancioff, *Phys. Rev. B* **33**, 1904 (1986); P. Stancioff, C. R. Willis, M. El-Batanouny, and S. Burdick, *ibid.* **33**, 1912 (1986).
- [3] P. Woafó, T. C. Kofané, and A. S. Bokosah, *J. Phys.: Condens. Matter* **3**, 2279 (1991) **4**, 809 (1992); **5**, 7063 (1993); *Phys. Rev. B* **48**, 10 153 (1993).
- [4] C. M. Ngabireng, P. Woafó, and T. C. Kofané, *Solid State Commun.* **89**, 885 (1994).
- [5] D. A. Bruce, *J. Phys. C* **13**, 4615 (1980).
- [6] F. Axel and S. Aubry, *J. Phys. C* **14**, 5433 (1981).
- [7] M. Peyrard and M. Remoissenet, *Phys. Rev. B* **26**, 2886 (1982).
- [8] Y. Ishibashi and I. Suzuki, *J. Phys. Soc. Jpn.* **53**, 4250 (1984).
- [9] P. Woafó, T. C. Kofané, and A. S. Bokosah, *Phys. Scr.* **56**, 655 (1997).
- [10] M. Remoissenet and M. Peyrard, *J. Phys. C* **14**, L481 (1981).
- [11] P. Prelovseh and I. Sega, *J. Phys. C* **14**, 5609 (1981).
- [12] Y. Ishibashi, *J. Phys. Soc. Jpn.* **46**, 1254 (1979).
- [13] D. A. Bruce, *J. Phys. C* **14**, 5195 (1981).
- [14] O. M. Braun, Yu. S. Kivshar, and I. I. Zelenskaya, *Phys. Rev. B* **41**, 7118 (1990).
- [15] O. M. Braun and M. Peyrard, *Phys. Rev. B* **51**, 17 158 (1995).
- [16] O. M. Braun, T. Dauxois, and M. Peyrard, *Phys. Rev. B* **54**, 313 (1996).
- [17] D. Yemélé and T. C. Kofané, *Phys. Rev. E* **56**, 1037 (1997).
- [18] T. C. Kofané, *J. Phys.: Condens. Matter* **11**, 2481 (1999).
- [19] D. Yemélé and T. C. Kofané, *Phys. Rev. B* **56**, 3353 (1997).
- [20] J. F. Currie, S. E. Trullinger, A. R. Bishop, and J. A. Krums-hanl, *Phys. Rev. B* **15**, 5567 (1977).